Received: 12 July 2024 | Revised: 9 October 2024 | Accepted: 11 November 2024

DOI: 10.1002/mrm.30386

TECHNICAL NOTE

Magnetic Resonance in Medicine

Single breath-hold volumetric lung imaging at 0.55T using stack-of-spiral (SoS) out-in balanced SSFP

Ye Tian[1] | **Nam G. Lee**[2] | **Ziwei Zhao**[1] | **Alison G. Wilcox**[3] | **Jorge J. Nieva**[4] | **Krishna S. Nayak**[1,2]

[1]Ming Hsieh Department of Electrical and Computer Engineering, Viterbi School of Engineering, University of Southern Calillrnia, Los Angeles, California, USA

[2]Department of Biomedical Engineering, Viterbi School of Engineering, University of Southern California, Los Angeles, California, USA

[3]Department of Radiology, Keck School of Medicine, University of Southern California, Los Angeles, California, USA

[4]Oncology Division, Keck School of Medicine, University of Southern California, Los Angeles, California, USA

Correspondence
Ye Tian, University of Southern California, 3740 McClintock Ave, EEB 406, Los Angeles, CA, 90089-2564, USA.
Email: ytian607@usc.edu

Funding information
National Heart, Lung, and Blood Institute, Grant/Award Numbers: R21HL159533, U01HL167613; Division of Computer and Network Systems, Grant/Award Number: 1828736

Abstract

Purpose: To develop a robust single breath-hold approach for volumetric lung imaging at 0.55T.

Method: A balanced-SSFP (bSSFP) pulse sequence with 3D stack-of-spiral (SoS) out-in trajectory for volumetric lung imaging at 0.55T was implemented. With 2.7× undersampling, the pulse sequence enables imaging during a 17-s breath-hold. Image reconstruction is performed using 3D SPIRiT and 3D l1-Wavelet regularizations. In two healthy volunteers, single breath-hold SoS out-in bSSFP was compared against stack-of-spiral UTE (spiral UTE) and half-radial dual-echo bSSFP (bSTAR), based on signal intensity (SI), blood-lung parenchyma contrast, and image quality. In six patients with pathologies including lung nodules, fibrosis, emphysema, and air trapping, single breath-hold SoS out-in and bSTAR were compared against low-dose computed tomography (LDCT).

Results: SoS out-in bSSFP achieved 2-mm isotropic resolution lung imaging with a single breath-hold duration of 17 s. SoS out-in (2-mm isotropic) provided higher lung parenchyma and blood SI and blood-lung parenchyma contrast compared to spiral UTE ($2.4 \times 2.4 \times 2.5\,mm^3$) and bSTAR (1.6-mm isotropic). When comparing SI normalized by voxel size, SoS out-in has lower lung parenchyma signal, higher blood signal, and a higher blood-lung parenchyma contrast compared to bSTAR. In patients, SoS out-in bSSFP was able to identify lung fibrosis and lung nodules of size 4 and 8 mm, and breath-hold bSTAR was able to identify lung fibrosis and 8 mm nodules.

Conclusion: Single breath-hold volumetric lung imaging at 0.55T with 2-mm isotropic spatial resolution is feasible using SoS out-in bSSFP. This approach could be useful for rapid lung disease screening, and in cases where free-breathing respiratory navigated approaches fail.

KEYWORDS

0.55 tesla, bSSFP, lung imaging, spiral out-in

Preliminary versions of this work were presented at the 2023 ISMRM Workshop on Data Sampling & Image Reconstruction, and the 2023 ISMRM Scientific Sessions, Abstract #1409.

1 | INTRODUCTION

Diagnostic imaging of the lung has been dominated by CT, which provides fast and high-quality images with exceptionally fine spatial resolution.[1] However, a significant concern with CT is the exposure to ionizing radiation, which can increase the risk of cancer,[2] particularly in the pediatric population. MRI, without ionizing radiation, can provide diagnostic lung imaging, but is challenging due to the low proton density in lung tissue and the short T_2 and T_2* relaxation times.

To address these challenges, UTE sequences[3,4] are typically used. By employing a truncated RF excitation followed by a center-out readout, these sequences have extremely short TEs, which can capture MR signal before it decays. UTE sequences have been used in many applications on 1.5 and 3T scanners such as evaluation of lung function,[5] nodule detection,[6] and assessment of structural defects.[7–9] Alternatively, balanced SSFP (bSSFP) sequences have been developed for lung structural imaging at 1.5T,[3,4,10] offering a much higher SNR compared to UTE sequences. These sequences require ultra short TR close to 1 ms to reduce banding artifacts at conventional field strengths.

Contemporary 0.55T MRI systems have shown great potential for improved lung MRI.[11–14] This is primarily due to reduced susceptibility effects,[15] more homogeneous B0 field, and prolonged T_2 and T_2* relaxations times.[13] UTE and bSSFP pulse sequences have been evaluated at 0.55 T. Self-navigated spiral UTE sequences have been developed,[16,17] achieving 1.75-mm isotropic resolution in 8.5 min. Free-breathing 0.55T bSSFP half-radial dual-echo (bSTAR) has also been demonstrated to image lung with submillimeter isotropic resolution in 13 min.[11] These sequences require continuous free-breathing acquisitions with self-navigation to obtain images with sufficient SNR. This approach relies on a regular breathing pattern, which cannot be guaranteed in patients with impaired lung function.

Single breath-hold volumetric lung imaging could offer more consistent image quality and is easily repeated if necessary. The duration of such scans needs to be within the patient's breath-hold capability, usually under 20 s. This requires efficient k-space coverage and high SNR efficiency. At 0.55T, reduced off-resonance effects and prolonged T_2 and T_2*[13] allow a longer bSSFP TR and readout duration without artifacts or dephasing. We hypothesize that single breath-hold volumetric lung imaging is possible at 0.55T by using bSSFP with an efficient spiral readout.

In this work, we propose a bSSFP 3D stack-of-spiral out-in pulse sequence, denoted SoS out-in, for single breath-hold volumetric lung imaging at 0.55T. We compare this against spiral UTE and bSTAR, on healthy volunteers with similar breath-hold durations. Image quality, and SI in parenchyma and blood are compared. We evaluate breath-hold SoS out-in and bSTAR in six patients with known lung nodules, using low-dose CT (LDCT) as the diagnostic reference.

2 | METHODS

2.1 | Spiral out-in trajectory design

The pulse sequence was optimized for both sampling efficiency and undersampling flexibility. A non-selective 80 μs hard pulse RF was used, followed by an SoS out-in readout. Figure 1A,B illustrates the pulse sequence and readout trajectory. The design of the spiral out-in readout is based on the method detailed in Tian et al.[18] First, a single spiral-out trajectory is designed to fully sample a $48 \times 48\,cm^2$ FOV with 120 interleaves, resulting in a readout time (T_{read}) of 1 ms. Next, the end of the spiral-out trajectory is modified to facilitate a smooth transition to the spiral-in trajectory by slowing down the gradient along the radial direction to zero. This modified spiral-out trajectory is then time reversed to form a spiral-in trajectory, and the two are concatenated to create a k_x, k_y spiral out-in trajectory with $T_{read} = 2$ ms. Cartesian phase encoding along the k_z direction is perfomed with 120 partitions. Duyn's method[19] was used to measure the actual spiral out-in trajectory, accounting for gradient system imperfections.

2.2 | Sampling scheme

The 3D SoS out-in trajectory allows for flexible undersampling, by varying the undersampling in both the k_x-k_y plane and along the k_z partition. The undersampling scheme used in this study is illustrated in Figure 1C. The central 20 k_z partitions are fully sampled to support SPIRiT reconstruction.[20] Peripheral k_z partitions are undersampled, by employing a two-fold k_x-k_y in-plane undersampling and 60% k_z partial Fourier. "Ping-pong" ordering along k_z is used to minimize imaging artifacts arising from eddy currents.[21] This resulted in 2.7× undersampling, corresponding to a breath-hold duration of 17 s. Breath-hold duration can also be reduced by using a coarser spatial resolution.[22]

2.3 | Image reconstruction

Image reconstruction uses both SPIRiT and 3D l_1-Wavelet regularizations. The SPIRiT regularization parameter is set to 2, and the Wavelet regularization parameter is set to

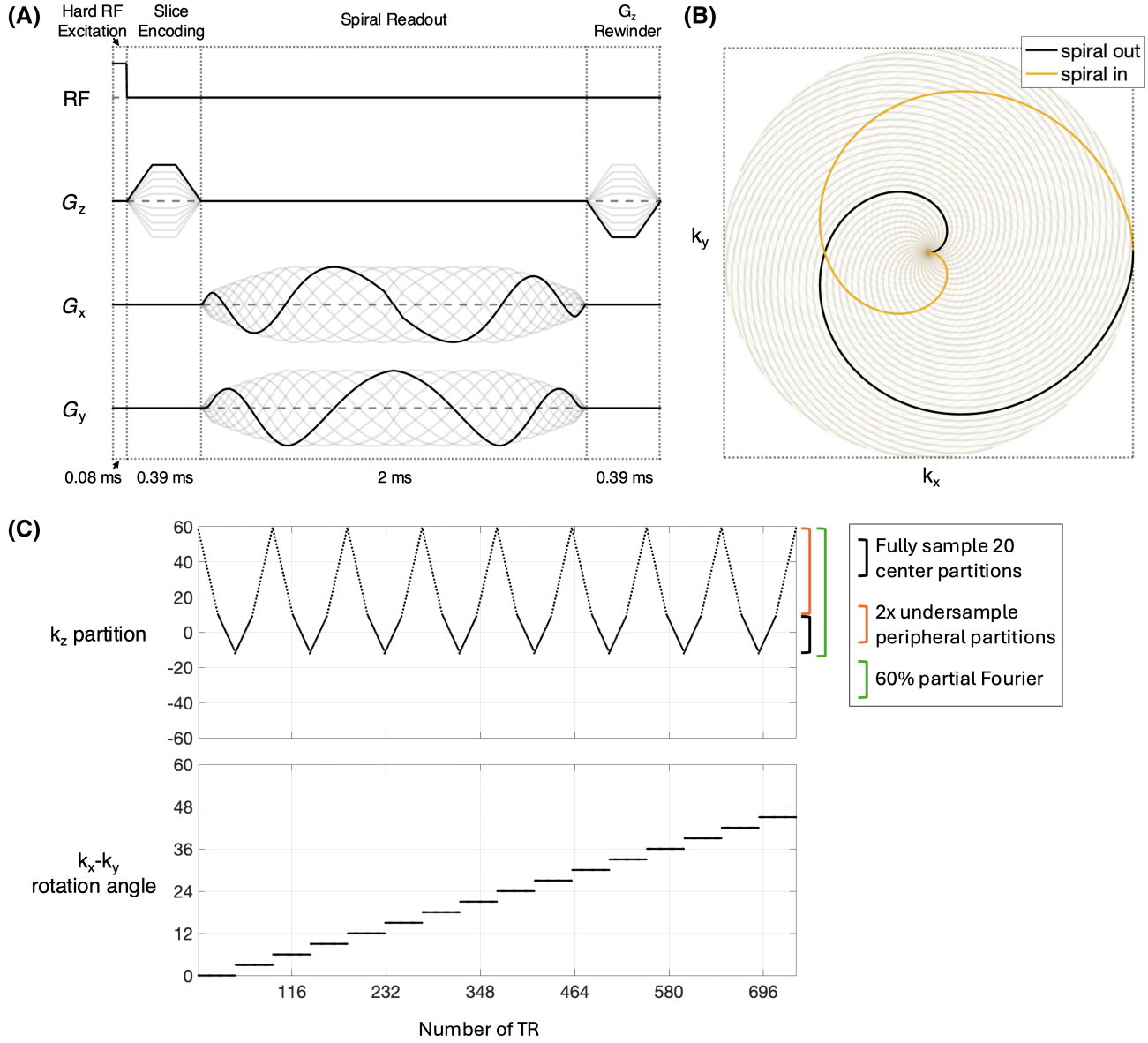

FIGURE 1 (A) bSSFP SoS out-in pulse sequence diagram. The pulse sequence is consistent of a hard RF excitation (0.08 ms), followed by k_z slice encoding (0.39 ms), a spiral out-in readout (2 ms), and a Gz rewinder (0.39 ms). Small delays between these modules are added in practice (not shown in diagram) to prevent potential overlapping due to system imperfection, resulting in a TR of 3.1 ms and a duty cycle of 70%. (B) Spiral out-in trajectory in the k_x-k_y plane. The spiral out-in readout is self M0-nulled and M1-nulled and does not slow down the entire gradient in the transition period, achieving a high sampling efficiently. (C) 3D undersampling pattern. Figures show the k_z partition (top) and k_x-k_y sampling angle (bottom) of the first 736 TRs. The fully sampled k-space has 120 k_z partitions, and each partition has 120 spiral arms uniformly distributed over the 360° angle. The illustrated sampling pattern is fully sampling center 20 k_z partitions, and undersample two times in all other k_z partitions, with an 60% partial Fourier along the k_z direction. This sampling pattern can be flexible in terms of k_x-k_y undersampling, calibration k_z partitions, and k_z partial Fourier.

0.002, based on previous experience.[11,20] The same method is applied to reconstruct spiral UTE images. For bSTAR reconstruction, we use the open-source implementation as described in Lee et al.[23] Noise-only data were acquired to allow the estimation of the noise correlation matrix for pre-whitening the multi-coil data. k-Space was scaled so the noise SD was 1.[24] This allowed for SI comparisons between sequences.

2.4 | Data acquisition

Data were collected on a whole-body 0.55T system (prototype MAGNETOM Aera, Siemens Healthineers) equipped with high-performance shielded gradients (45 mT/m amplitude, 200 T/m/s slew rate).[12] The study was approved by our institutional review board, and all subjects provided written informed consent. Two healthy volunteers (40/M

and 36/M) were scanned with 17-s single breath-hold SoS out-in, spiral UTE,[8] and bSTAR[23] sequences, during exhalation. Six patients (70 ± 9 y, three females and three males) were scanned during a 17-s breath-hold SoS out-in and bSTAR. Patients were instructed to perform exhale breath-hold, and to continue shallow breathing if no longer able to hold their breath. One patient was scanned with inhale breath-hold (Patient 2). Patients had confirmed lung pathologies by LDCT were recruited, which included nodules, fibrosis, air trapping, and emphysema. The standard-of-care clinical LDCT reports were considered as the gold standard reference when evaluating MRI images.

Details of breath-hold bSTAR and spiral UTE implementations can be found in Lee et al.[23] and Fauveau et al.,[8] respectively. While maintaining the scan time constant and other parameters matched as closely as possible, imaging parameters for the three sequences were as follows. SoS out-in: flip angle 25°, FOV $48 \times 48 \times 24\,cm^3$ (k_z encoding along the anterior–posterior direction with 24 cm FOV), spatial resolution 2-mm isotropic, TR/TE1/TE2 = 3.11/0.43/2.43 ms, with 80 dummy pulses in the beginning to stabilize the magnetization. bSTAR: flip angle 25°, FOV $36 \times 36 \times 36\,cm^3$ (without readout oversampling), spatial resolution 1.6-mm isotropic, TR/TE1/TE2 = 1.38/0.13/1.17 ms, 100 dummy pulses, 13 000 half-radial spokes, and four interleaves with wobbling Archimedean spiral pole sampling. Patient 1 was acquired with a bSTAR implementation in the vender platform[11] while the rest datasets were acquired with the open-source implementation.[23] Spiral UTE: flip angle 5°, FOV $48 \times 48 \times 24\ cm^3$, voxel size $2.5 \times 2.5 \times 2.4\,mm^3$, TR/TE = 4.34/0.03 ms, number of spiral arms per partition = 48, 72% partial Fourier along k_z. In one larger subject (Patient 4), SoS out-in was acquired with a FOV of $48 \times 48 \times 26\,cm^3$ and a voxel size of $2 \times 2 \times 2.17\,mm^3$ to cover all signal generating area, avoiding aliasing.

2.5 | Evaluation

In two healthy volunteers, SI between bSTAR, spiral UTE, and SoS out-in were compared. A lung region-of-interest (ROI) was defined semi-automatically using region-growing, followed by manual refinement. The average and SD of pixel SI within this ROI were reported as the lung parenchyma SI. An ROI was manually drawn in the descending aorta to calculate the mean and SD of the blood SI. This process was done for bSTAR and SoS out-in images in five patients where breath-hold bSTAR was acquired with the open-source implementation[23] (Patient 1 was excluded). SI between bSTAR and SoS out-in of two volunteers and five patients ($N = 7$) were evaluated by T-test. For patients, clinical LDCT reports were used to guide the review of MRI images.

3 | RESULTS

Demographic information for all subjects, including LDCT and MRI findings, are summarized in Table S1.

3.1 | Evaluation in healthy volunteers

Figure 2 shows a comparison of 17-s breath-hold SoS out-in, bSTAR, and spiral UTE at different maximum intensity projections (MIP). Both SoS out-in and bSTAR provide sufficient SNR and image contrast to visualize vessels and other structures in the lung, outperforming spiral UTE. SoS out-in has a higher apparent contrast between blood and lung parenchyma compared against bSTAR. However, bSTAR was acquired with a finer nominal spatial resolution (1.6-mm isotropic) than SoS out-in (2-mm isotropic), offering slightly better vessel definition.

3.2 | Evaluation in patients

Findings from LDCT, breath-hold SoS out-in, and breath-hold bSTAR are summarized in Table S1. Radiologist readings from LDCT confirmed three large nodules (one 4 mm and two 8 mm), and each was identified from a different patient. More than five small nodules (<4 mm) were identified. Several small, calcified granulomata (<4 mm) were also identified. Other identified lung conditions include lung fibrosis or scaring ($N = 2$), emphysema ($N = 3$), and air trapping ($N = 3$).

Both breath-hold SoS out-in and bSTAR were able to identify lung fibrosis and 8-mm nodules, with examples shown in Figure 3. Specifically, lung fibrosis was visible in two patients with both examples are shown in Figure 3(A,B). Two 8-mm nodules were visible in both sequences and one example is shown in Figure 3C. Breath-hold bSTAR has a lower apparent contrast compared with SoS out-in, resulting in worse definition of small blood vessels and other small structures.

SoS out-in was able to capture a 4-mm nodule as shown in Figure 4 whereas breath-hold bSTAR failed to identify the same nodule. Both breath-hold SoS out-in and bSTAR failed to capture nodules or calcified granulomata below 4 mm in size. Both breath-hold SoS out-in and bSTAR failed to identify emphysema or air trapping.

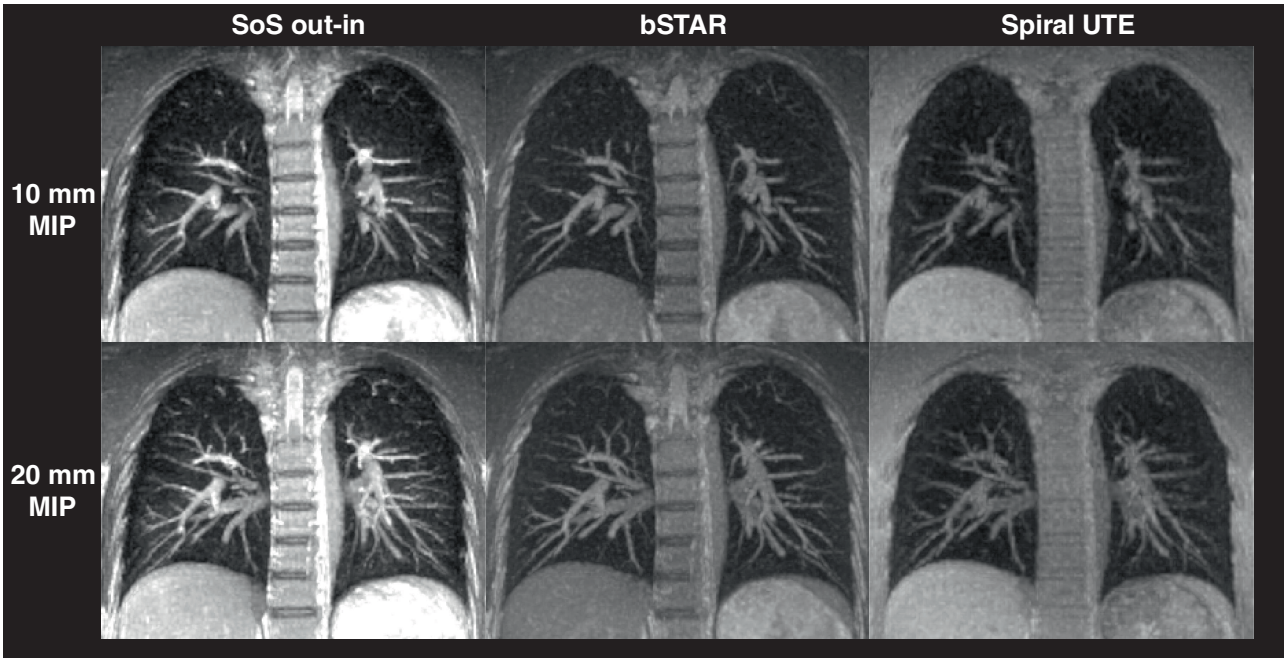

FIGURE 2 Comparison of SoS out-in, bSTAR, and spiral UTE in one healthy volunteer with different MIP. All sequences were acquired with a single 17-s breath-hold. The spiral UTE images had the worst image quality for depicting the lung vessels and lung parenchyma. Both SoS out-in and bSTAR sequences provided similar details of smaller lung vessels. However, SoS out-in had a higher contrast between blood vessels and lung parenchyma, whereas bSTAR had apparent sharper details, likely due to its finer acquisition voxel size. The images are displayed with the lung parenchyma signal normalized to the same level.

3.3 | Blood and lung parenchyma SI and contrast analysis

Figure 5(A,B) show the SI and contrast comparison between 17-s breath-hold SoS out-in, bSTAR, and spiral UTE in two healthy volunteers. Figure 5C shows normalized SI and contrast comparison of SoS out-in and bSTAR in two healthy volunteers and five patients. SoS out-in shows the highest SI in both lung parenchyma and blood. SoS out-in had a 1.95 times larger voxel size than bSTAR; when considering SI normalized by voxel size, bSTAR had higher lung parenchyma SI ($0.99/mm^3$) than SoS out-in ($0.58/mm^3$) ($p = 0.01$), however, the blood SI is significantly higher in SoS out-in ($3.03/mm^3$) than bSTAR ($2.66/mm^3$) ($p = 0.003$), resulting in much higher contrast in SoS out-in ($2.45/mm^3$) than bSTAR ($1.68/mm^3$) ($p = 1e\text{-}4$).

4 | DISCUSSION

We have developed a novel approach for high-quality single breath-hold volumetric lung imaging at 0.55T. With a mild 2.7 times undersampling SoS out-in bSSFP can capture the entire lungs with 2-mm isotropic resolution within a single breath-hold of 17 s. Compared to breath-hold versions of bSTAR and spiral UTE, SoS out-in provides significantly higher SI and image contrast. Its scan efficiency means that it minimizes reliance on regularization which can often cause artifacts. In patients, SoS out-in was able to identify lung nodules ≥4 mm and lung fibrosis, comparable to LDCT.

In the healthy volunteer experiment, the single breath-hold spiral UTE had a much lower SI and contrast than that of the bSSFP sequences. Although UTE sequences are widely used in lung imaging at 1.5 and 3T MRI,[8,9,25,26] using ultra-short TE may not be necessary at 0.55T as T2* in the lung is much longer.[13] For structural lung imaging at 0.55 T, bSSFP sequences may be advantageous than UTE sequences as they provide a higher SNR to reveal more detailed structures.[11] With the addition of magnetization preparation pulses, bSSFP may provide other imaging contrasts such as diffusion, T_1, or T_2 weighting. SoS out-in can provide single breath-hold volumetric imaging for other organs albeit it needs to be specifically optimized for each application.

Comparing the single breath-hold SoS out-in and bSTAR, a large SI difference was found which was primarily due to differences in voxel size. When normalizing SI by the voxel size, bSTAR had higher lung parenchyma SI, and SoS out-in had higher blood SI. This is partially attributed to the TR difference and the intravoxel dephasing.[4,10,27]

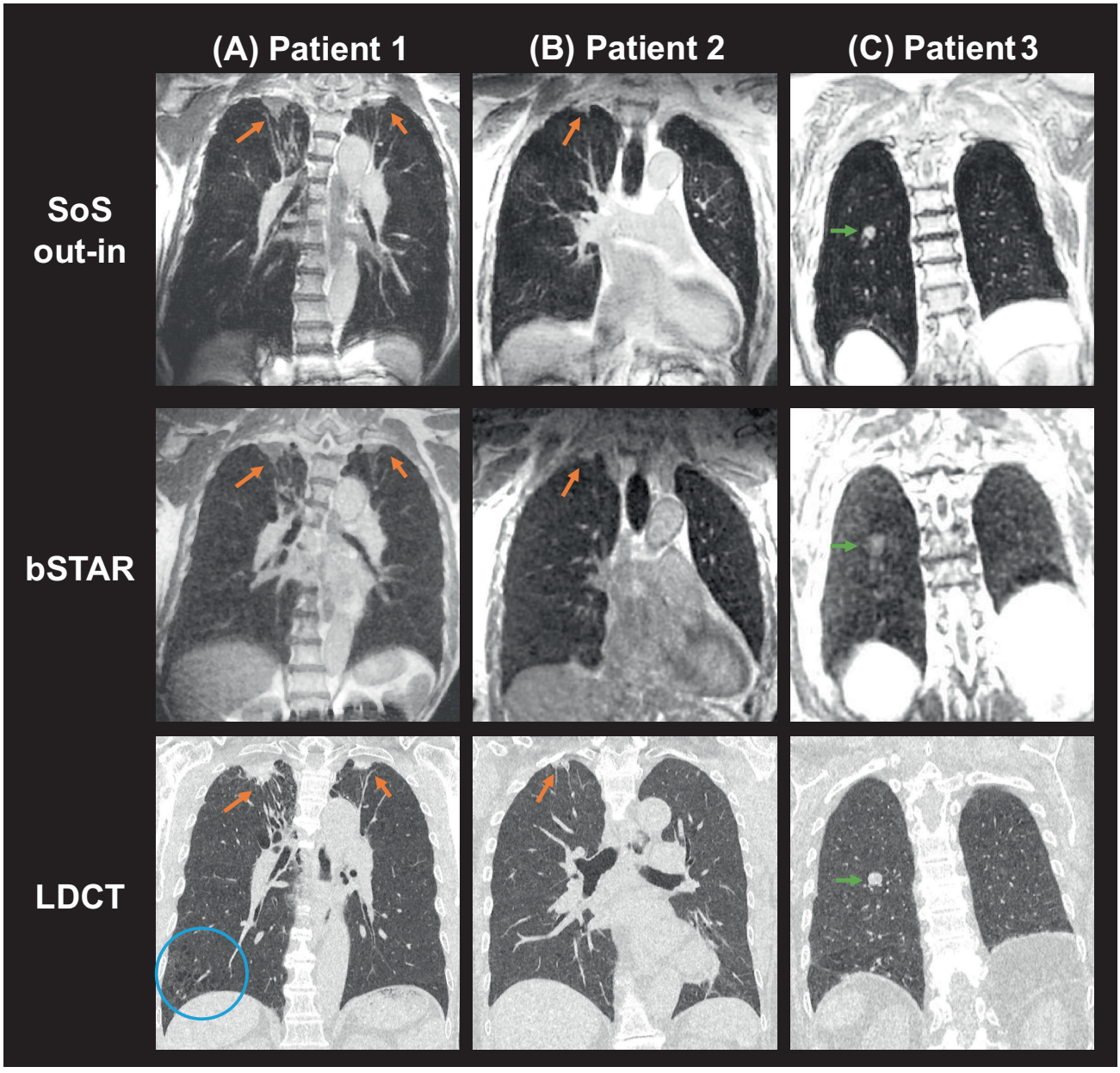

FIGURE 3 Representative examples of SoS out-in and bSTAR for identifying lung conditions in three patients. Patient 1 (74-y-old male) had bilaterial fibrosis in the superior lobes visible on both SoS out-in and bSTAR images (orange arrows). LDCT shows air trapping in the lower right lobe (blue circle), which is not identified on either MRI image. Patient 2 (80-y-old female) had fibrosis in the right upper lobe, visible in both SoS out-in and bSTAR images (orange arrow). Patient 3 (79-y-old female) had an 8-mm nodule, visible on both SoS out-in and bSTAR images (green arrow). All SoS out-in and bSTAR images were acquired with a 17-s breath-hold. In all patients, SoS out-in provide more detailed depictions of lung vessels and better blood-lung parenchyma contrast than bSTAR.

We also note the lower undersampling factor in SoS out-in than bSTAR. bSTAR uses radial sampling with an isotropic FOV, whereas SoS out-in uses a non-isotropic FOV that only covers the lung area (smaller in the anterior–posterior direction) and has a higher k-space sampling efficiency with spiral trajectory. SoS out-in had a Nyquist undersampling factor of 2.7 whereas bSTAR had an undersampling factor of 11.8 at the same 17-s breath-hold. This reduces the reliance on regularization and its possible impact on image quality,[28,29] enabeling the capture of smaller structures. This is reflected in the different abilities of SoS out-in and bSTAR in capturing a 4 mm nodule.

In this study, SoS out-in was implemented on a 0.55T scanner with high-performance gradient system, with 45 mT/m peak gradient and 200 T/m/s peak slew rate. For the sequence design, we used a peak gradient of 24 mT/m and peak slew rate of 180 T/m/s. When implementing SoS out-in sequence to commercially available 0.55T scanners

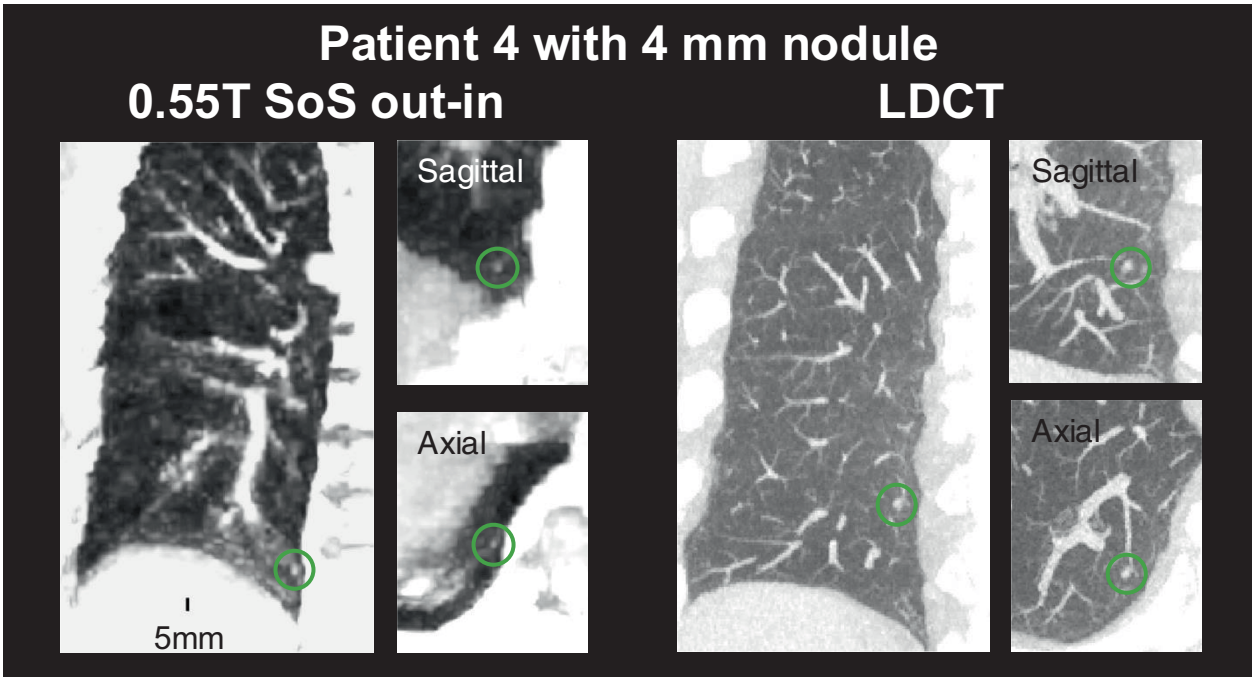

FIGURE 4 Orthogonal reformats of a 4-mm nodule in a 65-y-old female lung cancer patient. Images are displayed with a 10-mm MIP at three orthogonal reformats. The 4-mm nodule is marked by green circles on SoS out-in images (left) and LDCT images (right). The nodule location mismatch between the SoS out-in and LDCT is likely due to patient position (standing for LDCT and laying for MRI) and breath-hold instructions (inhale for LDCT and exhale in MRI). bSTAR (not shown) was unable to visualize this 4-mm nodule.

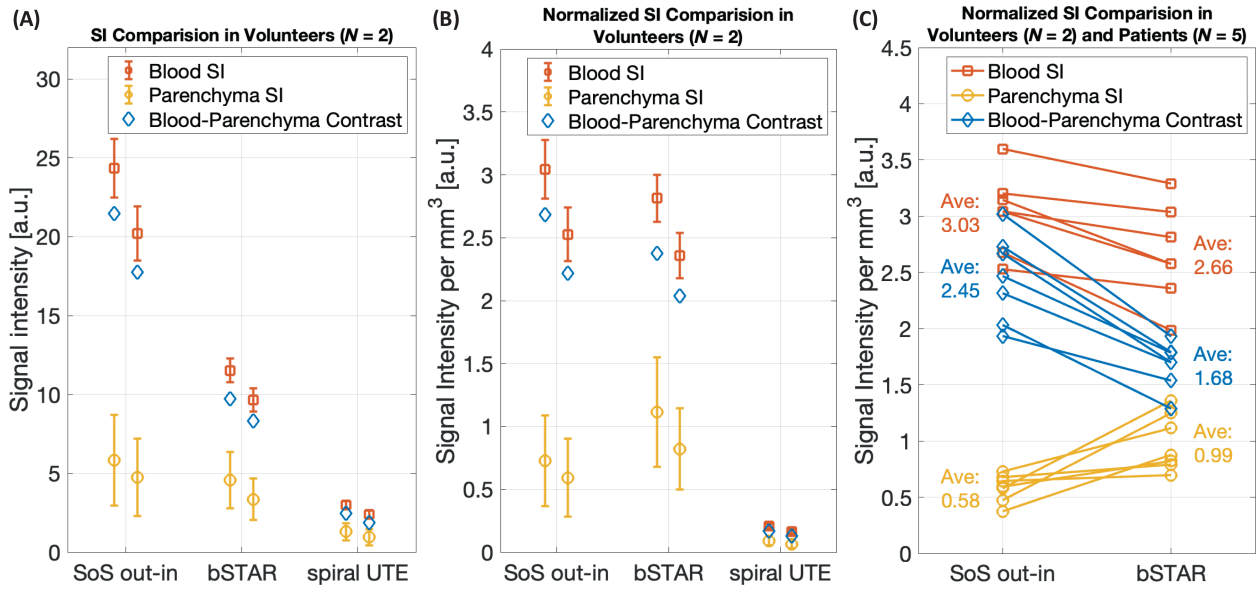

FIGURE 5 SI and contrast comparison between SoS out-in, bSTAR, and spiral UTE. SI was measured for both blood (in the descending aorta) and for lung parenchyma. (A) In two volunteers, spiral UTE had the overall lowest SI and contrast. SoS out-in had a higher SI and absolute contrast than bSTAR mainly due to a larger voxel size (1.95 times larger). (B) When normalizing SI by the voxel size, lung parenchyma SI was higher in bSTAR, but SoS out-in had a higher blood SI, resulting in greater contrast between blood and lung parenchyma in SoS out-in than bSTAR. (C) Comparing the normalized SI and contrast between SoS out-in and bSTAR in seven subjects, SoS out-in has statistically significant higher blood SI, lower lung parenchyma SI, and greater contrast than those of bSTAR.

with 26 mT/m peak gradient and 45 T/m/s peak slew rate, at the same 17-s breath-hold duration, the TR will be prolonged 5.78 ms and the undersampling factor will increase to 6.1. SoS out-in may need further optimization before applying on such platforms.

This study has limitations. First, patient evaluation was only performed in six subjects from our lung cancer screening cohort. A larger study is needed to establish diagnostic accuracy, sensitivity, or specificity. Another limitation is that we used LDCT readings to guide the MRI readings. Ideally, the MRI review should be conducted in a blinded fashion. However, at the pilot stage, radiologists preferred to confirm nodules with guidance from LDCT reports.

Opportunities exist in further improvements in the sampling scheme. The SoS out-in image quality degraded towards the diaphragm, which may be attributed to gradient nonlinearity, off-resonance, concomitant field, or breath-hold failure. Off-resonance and concomitant field issues are likely increased at a distance farther away from the magnet iso-center and near air-tissue boundaries. The ideal TR that is suitable for bSSFP lung imaging may be further optimized: a short TR is less efficient but could avoid issues such as banding artifacts from off-resonance, local blurring due to concomitant fields, or intravoxel dephasing.[4,10] As studied in Fauveau et al.,[8] a sampling scheme that fills the 3D k-space partition-by-partition may result in improved image quality for patients with compromised breath-hold capability. This may be adapted to the SoS out-in to improve its robustness against breath-hold failure and to study the trade-offs with eddy current artifacts.

5 | CONCLUSIONS

SoS out-in bSSFP at 0.55T is able to provide 2-mm isotropic volumetric lung imaging in a single breath hold at 17 s. SoS out-in bSSFP showed the capability of detecting lung nodules ≥4 mm and lung fibrosis.

DATA AVAILABILITY STATEMENT

Source code and sample raw data is provided at https://github.com/usc-mrel/breath_hold_sosoi upon acceptance. The data that support the findings of this study are openly available in Figshare at https://doi.org/10.6084/m9.figshare.27080503.v1.

ORCID

Ye Tian https://orcid.org/0000-0002-8559-4404
Nam G. Lee https://orcid.org/0000-0001-5462-1492
Ziwei Zhao https://orcid.org/0000-0003-0281-1141
Krishna S. Nayak https://orcid.org/0000-0001-5735-3550

REFERENCES

1. Jonas DE, Reuland DS, Reddy SM, et al. Screening for lung cancer with low-dose computed tomography: updated evidence report and systematic review for the US preventive services task force. *JAMA*. 2021;325:971-987.
2. Cao CF, Ma KL, Shan H, et al. CT scans and cancer risks: a systematic review and dose-response meta-analysis. *BMC Cancer*. 2022;22:1238.
3. Bieri O, Pusterla O, Bauman G. Free-breathing half-radial dual-echo balanced steady-state free precession thoracic imaging with wobbling Archimedean spiral pole trajectories. *Z Med Phys*. 2022;33:220-229.
4. Bauman G, Bieri O. Balanced steady-state free precession thoracic imaging with half-radial dual-echo readout on smoothly interleaved archimedean spirals. *Magn Reson Med*. 2020;84:237-246.
5. Heidenreich JF, Weng AM, Metz C, et al. Three-dimensional ultrashort echo time MRI for functional lung imaging in cystic fibrosis. *Radiology*. 2020;296:191-199.
6. Ohno Y, Takenaka D, Yoshikawa T, et al. Efficacy of ultrashort echo time pulmonary MRI for lung nodule detection and lung-RADS classification. *Radiology*. 2022;302:697-706.
7. Dournes G, Yazbek J, Benhassen W, et al. 3D ultrashort echo time MRI of the lung using stack-of-spirals and spherical k-space coverages: evaluation in healthy volunteers and parenchymal diseases. *J Magn Reson Imaging*. 2018;48:1489-1497.
8. Fauveau V, Jacobi A, Bernheim A, et al. Performance of spiral UTE-MRI of the lung in post-COVID patients. *Magn Reson Imaging*. 2023;96:135-143.
9. Geiger J, Zeimpekis KG, Jung A, Moeller A, Kellenberger CJ. Clinical application of ultrashort echo-time MRI for lung pathologies in children. *Clin Radiol*. 2021;76:708-708.e17.
10. Bieri O. Ultra-fast steady state free precession and its application to in vivo (1)H morphological and functional lung imaging at 1.5 tesla. *Magn Reson Med*. 2013;70:657-663.
11. Bauman G, Lee NG, Tian Y, Bieri O, Nayak KS. Submillimeter lung MRI at 0.55 T using balanced steady-state free precession with half-radial dual-echo readout (bSTAR). *Magn Reson Med*. 2023;90:1949-1957.
12. Campbell-Washburn AE, Ramasawmy R, Restivo MC, et al. Opportunities in interventional and diagnostic imaging by using high-performance low-field-strength MRI. *Radiology*. 2019;293:384-393.
13. Li B, Lee NG, Cui SX, Nayak KS. Lung parenchyma transverse relaxation rates at 0.55 tesla. *Magn Reson Med*. 2023;89:1522-1530.
14. Campbell-Washburn AE. 2019 American Thoracic Society BEAR cage winning proposal: lung imaging using high-performance low-field magnetic resonance imaging. *Am J Respir Crit Care Med*. 2020;201:1333-1336.
15. Schenck JF. The role of magnetic susceptibility in magnetic resonance imaging: MRI magnetic compatibility of the first and second kinds. *Med Phys*. 1996;23:815-850.

16. Javed A, Ramasawmy R, O'Brien K, et al. Self-gated 3D stack-of-spirals UTE pulmonary imaging at 0.55T. *Magn Reson Med*. 2022;87:1784-1798.
17. Javed A, Ramasawmy R, Ozenne V, Su P, Chow K, Campbell-Washburn A. Increasing the scan-efficiency of pulmonary imaging at 0.55 T using iterative concomitant field and motion-corrected reconstruction. *Magn Reson Med*. 2024;92:173-185.
18. Tian Y, Nayak KS. Real-time water/fat imaging at 0.55T with spiral out-in-out-in sampling. *Magn Reson Med*. 2023;91:649-659.
19. Duyn JH, Yang Y, Frank JA, van der Veen JW. Simple correction method for k-space trajectory deviations in MRI. *J Magn Reson*. 1998;132:150-153.
20. Lustig M, Pauly JM. SPIRiT: iterative self-consistent parallel imaging reconstruction from arbitrary k-space. *Magn Reson Med*. 2010;64:457-471.
21. Jung BA, Hennig J, Scheffler K. Single-breathhold 3D-trueFISP cine cardiac imaging. *Magn Reson Med*. 2002;48:921-925.
22. Ye T, Lee NG, Zhao Z, Nayak K. *Rapid 3D Lung Imaging with BSSFP Stack of Spiral out-in (SoSoi) Sampling At 0.55T*. Vol 2023. ISMRM; 2013:1409.
23. Lee NG, Bauman G, Bieri O, Nayak KS. Replication of the bSTAR sequence and open-source implementation. *Magn Reson Med*. 2024;91:1464-1477.
24. Kellman P, McVeigh ER. Image reconstruction in SNR units: a general method for SNR measurement†. *Magn Reson Med*. 2005;54:1439-1447.
25. Renz DM, Herrmann KH, Kraemer M, et al. Ultrashort echo time MRI of the lung in children and adolescents: comparison with non-enhanced computed tomography and standard post-contrast T1w MRI sequences. *Eur Radiol*. 2022;32:1833-1842.
26. Larson PEZ. Lung imaging with UTE MRI. 2023. p. arXiv:2312.00381.
27. Bieri O, Scheffler K. Fundamentals of balanced steady state free precession MRI. *J Magn Reson Imaging*. 2013;38:2-11.
28. Block KT, Uecker M, Frahm J. Undersampled radial MRI with multiple coils. Iterative image reconstruction using a total variation constraint. *Magn Reson Med*. 2007;57:1086-1098.
29. Ying L, Xu D, Liang ZP. On Tikhonov regularization for image reconstruction in parallel MRI. *Conf Proc IEEE Eng Med Biol Soc*. 2004;2004:1056-1059.

SUPPORTING INFORMATION

Additional supporting information may be found in the online version of the article at the publisher's website.

Table S1. Subject demographics and clinical findings.

How to cite this article: Tian Y, Lee NG, Zhao Z, Wilcox AG, Nieva JJ, Nayak KS. Single breath-hold volumetric lung imaging at 0.55T using stack-of-spiral (SoS) out-in balanced SSFP. *Magn Reson Med*. 2024;1-9. doi: 10.1002/mrm.30386